Numerical Methodologies for the Simulation of Liquid Metal Flows

V. Bellucci, S. Buono, G. Fotia, L. Maciocco,
V. Moreau, M. Mulas, G. Siddi, L. Sorrentino

1st October 1999

Contents

1 Introduction

The simulation of Liquid Metal Flows is becoming more and more important following the expansion of Research and Development in the field of Accelerator Driven Systems (ADS) and High Power Spallation Sources (HPSS). Numerical simulation often represents the unique tool to evaluate complex flow conditions as in the spallation target, where a complex heat source term is the consequence of the interaction between the proton beam and the Liquid Metal spallation material. Here we would like to review the basic methods implemented in the main Computational Fluid Dynamics (CFD) codes with a particular attention to numerical techniques, in order to validate the numerical simulation of flows of liquid metals characterised by high density and low Prandtl number.

The fluid dynamic modelling of the target and primary circuits of the Energy Amplifier Demonstration Facility (EADF) [1] is presented. The considered configuration is a liquid metal flow inside a container confined by a free surface. The flow is generated by buoyancy effects related to the heat produced by the nuclear reactions occurring inside the fluid. An additional external device (e.g. pumping systems or gas injection) may be used in order to enhance the natural circulation.

The study of this kind of flow can be performed by solving the Navier-Stokes equations with suitable initial and boundary conditions. These equations are first presented in their general form, then some simplifications are introduced, considering the low compressibility of liquids (low-Mach number flow) and the presence of the free surface.

A dimensional analysis is then performed and the dimensionless parameters governing the flow are identified. These parameters appear also in the dimensionless governing equations, allowing to compare the order of magnitude of different physical effects and to identify those that are negligible under specific flow conditions. In particular, the low-Mach number formulation of the Navier-Stokes equations can be obtained by expanding all the variables in power series of the Mach number and considering the limit when the Mach number approaches zero. With respect to the full Navier-Stokes equations, the low-Mach number formulation is characterised by the decomposition of the pressure in thermodynamic and dynamic pressures typical of the incompressible equations. The system of governing equations so obtained is the one usually employed in commercial codes for the simulation of liquid flows. Starting from the low-Mach formulation, further assumptions lead to more simplified models such as the Oberbeck-Boussinesq equations that are valid for low-Mach flows with small thermal variations.

In the second part of this work numerical schemes suitable for liquid flows are presented. The schemes we consider are based on the Finite Volumes spatial discretization usually employed in

Computational Fluid Dynamic (CFD) commercial codes. In such codes the time integration is performed by pressure-based approaches, i.e. the pressure is updated by a Poisson-like equation. Density-based schemes developed for compressible flows and extended to incompressible flows via preconditioning methods are also described.

2 Fluid Dynamics of Liquids

2.1 Navier-Stokes Governing Equations

The Navier-Stokes equations expressing the conservation of mass, momentum and total enthalpy are valid under the hypothesis of continuous medium (the molecular mean free path is much smaller than the characteristic length scale of the flow field). They read [2,3]

$$\frac{\partial \rho}{\partial t} + \nabla \cdot (\rho \, \underline{u}) = 0 \,, \tag{1}$$

$$\frac{\partial \rho \, \underline{u}}{\partial t} + \nabla \cdot (\rho \, \underline{u} \, \underline{u}) + \nabla \, p = \nabla \cdot \underline{\underline{\tau}} + \rho \, \underline{g} \,, \tag{2}$$

$$\frac{\partial}{\partial t} [\, \rho \, (h + K) \,] + \nabla \cdot [\, \rho \, (h + K) \, \underline{u} \,] = \frac{\partial p}{\partial t} + \nabla \cdot (\underline{\underline{\tau}} \cdot \underline{u}) + \nabla \cdot \underline{q} + \rho \, \underline{g} \cdot \underline{u} + Q \tag{3}$$

where t is the time, ρ the density, $\underline{u}$ the velocity, p the pressure, $\underline{\underline{\tau}}$ the stress tensor, $\underline{g}$ the gravity acceleration, e the internal energy, h the enthalpy, K the kinetic energy, $\underline{q}$ the heat flux and Q the heat generation per unit volume. In this work the gravity acceleration is supposed to be constant with $g = |\underline{g}| = 9.81 \, m \, s^{-2}$. The enthalpy and the kinetic energy are respectively defined as

$$h = e + \frac{p}{\rho} \,, \tag{4}$$

$$K = \frac{|\underline{u}|^2}{2} \,. \tag{5}$$

For a Newtonian fluid the stress tensor is given by

$$\underline{\underline{\tau}} = 2 \, \mu \, \underline{\underline{s}} + \left(\lambda - \frac{2}{3} \, \mu \right) (\nabla \cdot \underline{u}) \, \underline{\underline{I}} \tag{6}$$

where λ is the bulk viscosity, μ the viscosity, $\underline{\underline{I}}$ the unit tensor and

$$\underline{\underline{s}} = \frac{\nabla \, \underline{u} + \nabla \, \underline{u}^T}{2} \tag{7}$$

the strain-rate tensor. The bulk viscosity is found to be usually very small, except in presence of non-equilibrium phenomena as when vibrational modes of molecules are excited [2]. Therefore, the assumption $\lambda = 0$ generally holds.

The heat flux is expressed by the Fourier law as

$$\underline{q} = \eta \, \nabla \, T \tag{8}$$

where η is the thermal conductivity and T the temperature.

For liquids, the transport coefficients μ and η may be assumed to be functions of temperature only, being the dependence from the pressure usually negligible. Therefore,

$$\mu = \mu(T), \quad \eta = \eta(T). \tag{9}$$

Other forms of the energy equation may be also deduced. The equation for the kinetic energy is obtained by multiplying Eq. (2) by $\underline{u}$. It gives

$$\rho \frac{DK}{Dt} + \nabla \cdot (p\,\underline{u}) = p\nabla \cdot \underline{u} + \nabla \cdot (\underline{\underline{\tau}} \cdot \underline{u}) + \rho\,\underline{g} \cdot \underline{u} - \Phi \tag{10}$$

where $D/Dt = \partial/\partial t + \underline{u} \cdot \nabla$ is the Lagrangian derivative and

$$\Phi = \underline{\underline{\tau}} : \nabla \underline{u} \tag{11}$$

is the viscous dissipation.

The equation for the static enthalpy is obtained by subtracting Eq. (10) from Eq. (3). It yields

$$\rho \frac{Dh}{Dt} = \frac{\partial p}{\partial t} + \underline{u} \cdot \nabla p + \nabla \cdot \underline{q} + \Phi + Q. \tag{12}$$

The equation for the internal energy can be easily deduced from Eq (12) and Eq. (4), yielding

$$\rho \frac{De}{Dt} = -p\nabla \cdot \underline{u} + \nabla \cdot \underline{q} + \Phi + Q. \tag{13}$$

The temperature equation is obtained by using Eq. (13), Eq. (4) and the relation [4]

$$dh = C_p\,dT + \frac{1 - \beta T}{\rho}\,dp \tag{14}$$

where C_p is the specific heat at constant pressure and β the thermal-expansion coefficient defined as

$$\beta = -\frac{1}{\rho}\left(\frac{\partial \rho}{\partial T}\right)_p. \tag{15}$$

It yields

$$\rho C_p \frac{DT}{Dt} = \beta T \frac{Dp}{Dt} + \nabla \cdot \underline{q} + \Phi + Q. \tag{16}$$

The conservation equation for the entropy s is obtained by using Eq. (16) and the relation [4]

$$ds = \frac{C_p}{T}\,dT - \frac{\beta}{\rho}\,dp. \tag{17}$$

It reads

$$\rho T \frac{Ds}{Dt} = \nabla \cdot \underline{q} + \Phi + Q \,. \tag{18}$$

The system of governing equations is completed by the equations of state [4]

$$p = p(\rho, T), \tag{19}$$

$$e = e(\rho, T). \tag{20}$$

For liquids in defined ranges of temperature and pressure, the first equation of state (19) may be expressed as

$$\rho = \rho_0 - \alpha_T (T - T_0) + \alpha_p (p - p_0) \tag{21}$$

where the suffix 0 refers to quantities evaluated at a reference thermodynamic state included in the (T, p) application range. The two parameters α_T and α_p are constant and are given respectively by

$$\alpha_T = \rho\beta, \quad \alpha_p = \rho\chi \tag{22}$$

where χ is the isothermal coefficient of compressibility expressed as

$$\chi = \frac{1}{\rho}\left(\frac{\partial \rho}{\partial p}\right)_T . \tag{23}$$

The variables β and χ are connected to C_p, the specific heat at constant volume C_v and the speed of sound c by the relations [4]

$$c^2 = \frac{C_p}{C_v \rho \chi}, \tag{24}$$

$$C_p - C_v = \frac{\beta^2 T}{\rho \chi}. \tag{25}$$

Tab. 1 reports for different liquids the values of some thermodynamic variables.

By assuming negligible surface deformations, the free surface is simulated as a horizontal plane whose vertical position changes in time. The hydrostatic contribution to pressure may be eliminated by defining the modified pressure P as

$$P = p - p_0 - \rho_0 g [z - z_s(t)] \tag{26}$$

where the z-axis is directed along the $\underline{g}$ direction and $z_s(t)$ is the z-coordinate of the free surface [1]. Using this pressure, Eqs. (2) may be expressed as

$$\frac{\partial \rho \underline{u}}{\partial t} + \nabla \cdot (\rho \underline{u}\,\underline{u}) + \nabla P = \nabla \cdot \underline{\underline{\tau}} + (\rho - \rho_0)\underline{g}. \tag{27}$$

[1] The free surface position is determined through the global mass conservation equation.

Fluid	$\beta \times 10^6$ (K^{-1})	$\chi \times 10^{11}$ (Pa^{-1})	c $(m\,s^{-1})$	γ
Water at 20^oC, $1\,atm$	207	46	1482	1.01
Mercury at 0^oC, $1\,atm$	181	3.8	1470	1.12
Lead at melting point	124	3.4	1820	1.21

Table 1: : Thermal-expansion coefficient β, isothermal coefficient of compressibility χ, speed of sound c and specific heat ratio C_p/C_v for different liquids.

2.1.1 Initial and boundary conditions

The initial conditions for our problem may be assumed as the hydrostatic ones. Moreover, in Eq. (21) we can assume the 0-state as the initial solution state corresponding to the free-surface gravitational potential line. Therefore, the initial temperature field is assumed to be T_0 and $p_0 = p_s$ being p_s the uniform free-surface pressure. It yields

$$T\,(\,\underline{x}\,,\,t_{in}\,) = T_0\,, \quad P\,(\,\underline{x}\,,\,t_{in}\,) = P_{in}\,(\,z\,)\,, \quad \rho\,(\,\underline{x}\,,\,t_{in}\,) = \rho_{in}\,(\,z\,)\,, \quad \underline{u}\,(\,\underline{x}\,,\,t_{in}\,) = 0 \tag{28}$$

where $\underline{x}$ is the position vector and t_{in} the initial time. The functions $P_{in}(z)$ and $\rho_{in}(z)$ are solutions of the system formed by Eq. (21) and the differential equation (see Eq. (27))

$$\frac{dP}{dz} = -(\rho - \rho_0)\,g \tag{29}$$

where the starting condition for the integration is

$$P_{in}(0) = 0\,. \tag{30}$$

The boundary of the domain may be in general decomposed into the free surface $\partial\Omega_s$ and the adiabatic solid walls $\partial\Omega_a$. The boundary conditions for our problem are then expressed as

$$\underline{u}\cdot\underline{n} = 0 \quad \text{and} \quad P = 0 \quad \text{on } \partial\Omega_s\,, \tag{31}$$

$$\underline{u} = 0 \quad \text{and} \quad \nabla P\cdot\underline{n} + (\nabla\cdot\tau)\cdot\underline{n} = 0 \quad \text{on } \partial\Omega_a\,, \tag{32}$$

$$\nabla T\cdot\underline{n} = 0 \quad \text{on } \partial\Omega_s + \partial\Omega_a \tag{33}$$

where $\underline{n}$ is the normal to the boundaries.

2.1.2 Incompressible flows

Liquid flows are usually assumed as incompressible, i.e. the density is supposed to be independent of pressure. To investigate the validity of such hypothesis, we can correlate density variations to pressure and entropy variations by using the relation [4]

$$\frac{D\rho}{Dt} = \frac{1}{c^2}\frac{Dp}{Dt} - \frac{\rho\beta T}{C_p}\frac{Ds}{Dt}\,. \tag{34}$$

On the other hand, from Eq. (10) one has

$$\frac{Dp}{Dt} = \frac{\partial p}{\partial t} - \rho\frac{DK}{Dt} + \underline{u}\cdot\left(\nabla\cdot\underline{\underline{\tau}} + \rho\,\underline{g}\right) \tag{35}$$

showing that the contributes to pressure variations are due to: (i) unsteadiness of motion $\partial p/\partial t$; (ii) velocity variations of the fluid element (according to Bernoulli theorem) $\rho DK/Dt$; (iii) work of the viscous stress and viscous dissipation $\underline{u}\cdot(\nabla\cdot\underline{\underline{\tau}}) = \nabla\cdot(\underline{\underline{\tau}}\cdot\underline{u}) - \Phi$; (iv) work of the buoyancy force $\underline{u}\cdot\rho\underline{g}$. When all these contributes have a negligible effect on density variations, the flow is incompressible. Therefore the incompressibility condition can be obtained by assuming an infinite speed of sound in Eq. (34).

By making the divergence of Eq. (2) and using Eqs. (1), (21), (16), (24) and (25), the nonlinear pressure waves are found to be governed by the hyperbolic equation

$$\begin{aligned}\frac{\partial}{\partial t}\left(\frac{1}{c^2}\frac{\partial p}{\partial t}\right) - \nabla^2 p \;\;=\;\; & \nabla\cdot\left[\,\nabla\cdot(\rho\,\underline{u}\,\underline{u}) - \nabla\cdot\underline{\underline{\tau}} - \rho\,\underline{g}\,\right] \\ & + \frac{\partial}{\partial t}\left[\frac{\beta}{C_p}\left(-\rho\,C_p\,\underline{u}\cdot\nabla T + \beta\,T\,\underline{u}\cdot\nabla p + \nabla\cdot\underline{q} + \Phi + Q\right)\right]\end{aligned} \tag{36}$$

where the right-hand term represents the sources of pressure waves. A sound wave is generated when small (isentropic) perturbations occur in a fluid at rest [2,3], i.e. when density and pressure may be written as $\rho = \rho_0 + \hat{\rho}$ and $p = p_0 + \hat{p}$ with $\hat{\rho} \ll \rho_0$ and $\hat{p} \ll p_0$. Being the velocity of the order of magnitude of $\hat{\rho}$ and $\hat{p}$, the leading order expansion of Eq. (36) is given by

$$\frac{1}{c_0^2}\frac{\partial^2\hat{p}}{\partial t^2} - \nabla^2\hat{p} = -\frac{\underline{g}\cdot\nabla\hat{p}}{c_0^4}\,. \tag{37}$$

When pressure gradients are small compared with c_0^2/g, Eq. (37) reduces to the wave equation. When the speed of sound approaches infinity the pressure wave equation becomes the Laplace equation

$$\nabla^2\hat{p} = 0\,. \tag{38}$$

Eq. (38) shows that in the incompressible approximation the propagation mechanism of pressure wave is suppressed.

2.2 Dimensional Analysis

The dimensional analysis allows to re-write a relationship between the parameters which describe the physical phenomena as a relationship between a lower number of dimensionless numbers [5]. Flows having the same values of the dimensionless numbers are similar, i.e. the time-space distribution of their properties can be obtained one from another by means of a change of scales.

The physical parameters of the flow are those appearing in governing equations, initial data and boundary conditions. The initial data of our problem are T_0 and ρ_0 (see Eqs. (28) and (30)). The reference fluid properties are $\mu_0 = \mu(T_0)$, $\eta_0 = \eta(T_0)$, $C_{p0} = C_p(\rho_0, T_0)$, $\beta_0 = \beta(\rho_0, T_0)$ and $\chi_0 = \chi(\rho_0, T_0)$. These values are sufficient to characterise the fluid only if the laws relating the transport and thermodynamic properties of two different fluids to temperature are similar, as it is assumed for simplicity. The geometry scale of the vessel is characterised by the reference length L. The effects due to the heat source may be represented by means of a reference temperature difference ΔT defined as

$$\Delta T = \frac{Q_0 \, L}{\rho_0 \, C_{p0} \, V} \tag{39}$$

where Q_0 is the reference value of the heat source.

Then, velocity, pressure and density fields are functions of the following independent parameters

$$\underline{u} = f_u \left(\underline{x} \, , \, t \, , \, \rho_0 \, , \, T_0 \, , \, L \, , \, V \, , \, g \, , \, \Delta T \, , \, \mu_0 \, , \, \eta_0 \, , \, C_{p0} \, , \, \beta_0 \, , \, \chi_0 \right) , \tag{40}$$

$$p = f_p \left(\underline{x} \, , \, t \, , \, \rho_0 \, , \, T_0 \, , \, L \, , \, V \, , \, g \, , \, \Delta T \, , \, \mu_0 \, , \, \eta_0 \, , \, C_{p0} \, , \, \beta_0 \, , \, \chi_0 \right) , \tag{41}$$

$$T = f_T \left(\underline{x} \, , \, t \, , \, \rho_0 \, , \, T_0 \, , \, L \, , \, V \, , \, g \, , \, \Delta T \, , \, \mu_0 \, , \, \eta_0 \, , \, C_{p0} \, , \, \beta_0 \, , \, \chi_0 \right) . \tag{42}$$

The dimensional analysis is based on the invariance of physical laws with respect to the reference system and is represented by the π-theorem [5]. The total number of flow parameters on the right-hand side in the above equations is 13 while the number of primary dimensions is 4 (length, mass, time and temperature). According to the π-theorem, the dimensionless parameters which govern the flow are 13-4=9. They may be obtained by choosing L, V, ρ_0 and C_{p0} as parameters representing the four primary dimensions. As a result of the dimensional analysis we find that

$$\frac{\underline{u}}{V} = \pi_u \left(\underline{x}^* \, , \, t^* \, , \, Re \, , \, Gr \, , \, Pr \, , \, Ec \, , \, \gamma \, M^2 \, , \, \epsilon \, , \, \sigma \, , \right) , \tag{43}$$

$$\frac{p}{\rho_0 \, V^2} = \pi_p \left(\underline{x}^* \, , \, t^* \, , \, Re \, , \, Gr \, , \, Pr \, , \, Ec \, , \, \gamma \, M^2 \, , \, \epsilon \, , \, \sigma \, , \right) , \tag{44}$$

$$\frac{T}{V^2 / C_{p0}} = \pi_T \left(\underline{x}^* \, , \, t^* \, , \, Re \, , \, Gr \, , \, Pr \, , \, Ec \, , \, \gamma \, M^2 \, , \, \epsilon \, , \, \sigma \, , \right) \tag{45}$$

where the dimensionless parameters on the right-hand sides are

$$\underline{x}^* = \frac{\underline{x}}{L} \quad \text{(dimensionless length)},$$

$$t^* = \frac{t}{L/V} \quad \text{(dimensionless time)},$$

$$Re = \frac{\rho_0 V L}{\mu_0} \quad \text{(Reynolds number)},$$

$$Gr = \frac{\rho_0^2 L^3 g \beta_0 \Delta T}{\mu_0^2} \quad \text{(Grashof number)}.$$

$$Pr = \frac{\mu_0 C_{p0}}{\eta_0} \quad \text{(Prandtl number)},$$

$$Ec = \frac{V^2}{C_{p0} \Delta T} \quad \text{(Eckert number)},$$

$$\gamma = \frac{C_{p0}}{C_{v0}} \quad \text{(specific heats ratio)},$$

$$M = \frac{V}{c_0} \quad \text{(Mach number)},$$

$$\epsilon = \beta_0 \Delta T,$$

$$\sigma = \beta_0 T_0.$$

The Reynolds number represents the ratio between inertial forces and viscous forces. The Grashof number accounts for buoyancy effects. The Prandtl number depends on fluid properties only: in Tab.2 the values of Pr for different liquids are reported. The Prandtl number represents the ratio between the viscous diffusion rate (i.e. the kinematic viscosity $\nu = \mu/\rho$) and the thermal diffusion rate $\eta_0/(\rho_0 C_{p0})$. Hence, when Pr is of order one (as for water) the thickness of the kinematic and thermal boundary layers is the same. Liquid metals are characterised by values of Pr much smaller than one and consequently by thermal boundary layers thicker than the kinematic ones. The Eckert number is related to the ratio between the temperature increase due to an isentropic arrest of fluid and ΔT (in fact Eqs. (17), (2) and (10) written for a steady isentropic flow yield

Fluid	Molten lead	Mercury	Water	Oil	Glycerine
Pr	0.02	0.044	7	10^4	$1.2 \cdot 10^4$

Table 2: : Prandtl number for different liquids.

$C_p \Delta T = \beta T \Delta u^2/2$). The parameters ϵ and σ are connected to the similarity of the thermodynamic behaviour of the fluid. In particular, the equality of ϵ for two different flows means the equality of the isobaric relative density variations. In fact when $dp = 0$ in Eq. (21) one has that $\epsilon = \Delta\rho/\rho_0$. On the other hand, σ is seen to relate temperature differences and pressure differences in the isentropic case (from Eq. (17) with $ds = 0$ one has $\sigma = C_{p0}\Delta T/(\Delta p/\rho_0)$). Any other quantity is a function of the numbers listed above. For instance, the heat flux q_w per unit exchange surface between fluid and wall may be expressed by means of the heat transfer coefficient h_w defined by the expression

$$q_w = h_w \, \Delta T \, . \tag{46}$$

Therefore, the dimensionless number

$$Nu = \frac{h_w \, L}{\eta_0} \quad \text{(Nusselt number)}$$

is given by

$$Nu = \pi_{Nu} \left(\underline{x}^* \, , \, t^* \, , \, Re \, , \, Gr \, , \, Pr \, , \, Ec \, , \, \gamma \, M^2 \, , \, \sigma \, , \, \epsilon \right) \, . \tag{47}$$

2.3 Dimensionless Governing Equations

The dimensional analysis gives no information about the form of the functions π (i.e. the relationships in terms of the dimensionless parameters). So, the study of the asymptotic behaviour of π when one or more of the arguments assume a very large or a very small value, is not possible using only the dimensional analysis. For instance it will be shown in the following Section that when the Mach number approaches zero, the dependence of Eqs. (43)-(45) and (47) from γM^2 can be neglected. On the other hand if viscous forces are negligible with respect to inertial forces then $Re \to \infty$. However viscous terms must be retained because close to solid walls (in the boundary layer) inertial forces and viscous forces are of the same order of magnitude. To investigate the importance of the dimensionless parameters in a particular fluid flow, the dimensionless form of governing equations has to be considered.

The governing equations (1), (27), (16) and (21) may be written in dimensionless form by dividing the dimensional values by constant reference quantities supplied by the data (boundary conditions and initial solution) in order to have dimensionless terms ranging from zero to a value of the order one. We assume that the flow has a single time scale and a single length scale. Therefore, the following reference quantities are defined: V for fluid speed variations (velocity is zero on solid walls), L for length, L/V for time, ρ_0 for density, T_0 for temperature, μ_0 for viscosity, η_0 for thermal conductivity, Q_0 for heat source, β_0 for thermal-expansion coefficient, χ_0 for isothermal coefficient of compressibility, C_{p0} for specific heat at constant pressure and C_{v0} for specific heat at constant volume. In the following, dimensionless variables will be denoted by an asterisk. In Eq. (27) a proper dimensionless modified pressure is

$$P^* = \frac{P}{\rho_0 V^2}\,. \tag{48}$$

Eq. (21) may be written in the form (see Eqs. (15) and (24))

$$\rho = \rho_0 - \alpha_T (T - T_0) + \frac{\gamma}{c_0^2}(p - p_0) \tag{49}$$

showing that the dimensionless pressure in Eq. (49) should be

$$p^* = \frac{\gamma}{\rho_0\, c_0^2}(p - p_0) \tag{50}$$

in order to have a dimensionless equation of state independent of dynamical quantities (i.e. the fluid velocity). The dimensionless temperature difference θ is defined as

$$\theta = \frac{T - T_0}{\Delta T} = \frac{T_0}{\Delta T}(T^* - 1)\,. \tag{51}$$

By employing such reference quantities, the dimensionless system of governing equations (26), (1), (27), (16) and (49) is written in terms of dimensionless variables as

$$p^* = \gamma M^2 \left[P^* + \frac{Gr}{\epsilon\, Re^2}(z^* - z_s^*) \right]\,, \tag{52}$$

$$\frac{\partial \rho^*}{\partial t^*} + \nabla^* \cdot (\rho^*\, \underline{u}^*) = 0\,, \tag{53}$$

$$\frac{\partial \rho^*\, \underline{u}^*}{\partial t^*} + \nabla^* \cdot (\rho^*\, \underline{u}^*\, \underline{u}^*) + \nabla P^* = \frac{1}{Re}\nabla^* \cdot \underline{\underline{\tau}}^* + \frac{Gr}{\epsilon\, Re^2}(\rho^* - 1)\frac{\underline{\underline{g}}}{g}\,, \tag{54}$$

$$\rho^*\, C_p^* \frac{D\theta}{Dt^*} = \frac{\sigma\, Ec}{\gamma\, M^2}\beta^*\, T^* \frac{Dp^*}{Dt^*} + \frac{1}{Re\, Pr}\nabla^* \cdot (\eta^*\, \nabla^* \theta) + \frac{Ec}{Re}\Phi^* + Q^*\,, \tag{55}$$

$$\rho^* = 1 - \epsilon\,\theta + p^*\,. \tag{56}$$

The Prandtl number appears only in the product $Re\,Pr$ that is also called Peclet number.

2.4 Low-Mach Number Asymptotic Analysis

The low-Mach number governing equations are obtained by expanding all the dimensionless quantities ψ^* in asymptotic series of the form

$$\psi^* (\underline{x}^* , t^* , \gamma M^2) = \psi^{*(0)} (\underline{x}^* , t^*) + \gamma M^2 \psi^{*(1)} (\underline{x}^* , t^*) + \mathcal{O} \left[(\gamma M^2)^2 \right] \tag{57}$$

being in general γ a factor of order one (see Tab. 1). The low-Mach number expansion is obtained by inserting Eq. (57) into Eqs. (52)-(56) and by considering the limit $\gamma M^2 \to 0$. In the following the superscript $*$ will be dropped.

By expanding Eq. (52) one has at the zero-order

$$p^{(0)} = \frac{\gamma M^2 Gr}{\epsilon Re^2} (z - z_s) . \tag{58}$$

The term on the right-hand side of the above equation may be neglected if $\gamma M^2 Gr/(\epsilon Re^2) \ll 1$, i.e if

$$\frac{\gamma g L}{c_0^2} \ll 1 \tag{59}$$

that is verified when L is much smaller than the "scale height" $c_0^2/(\gamma g)$. Eq. (59) may be also written as $\chi_0 \rho_0 g L \ll 1$ being $\rho_0 g L$ the reference hydrostatic variation of pressure. Therefore, relative density variations due to the hydrostatic variation of pressure are supposed to be much smaller than one. $\epsilon Re^2/Gr$ may be of order M^2 in stellar or atmospheric circulation gas flows. For liquids the scale height is of the order of $100\,km$. Consequently Eq. (59) may be assumed valid for the EADF liquid metal flows and Eq. (58) can be written as

$$p^{(0)} = 0 . \tag{60}$$

The expanded form of Eq. (53) is given by

$$\frac{\partial \rho^{(0)}}{\partial t} + \nabla^* \cdot \left(\rho^{(0)} \underline{u}^{(0)} \right) = 0 . \tag{61}$$

When expanding Eq. (54), one has

$$\begin{aligned} \frac{\partial \rho^{(0)} \underline{u}^{(0)}}{\partial t} + \nabla^* \cdot \left(\rho^{(0)} \underline{u}^{(0)} \underline{u}^{(0)} \right) + \nabla P^{(0)} \quad = \quad & \frac{1}{Re} \nabla^* \cdot \underline{\underline{\tau}}^{(0)} - \frac{Gr}{Re^2} \theta^{(0)} \frac{\underline{\underline{g}}}{g} \\ & + \frac{\gamma M^2}{Re} \nabla^* \cdot \underline{\underline{\tau}}^{(1)} - \frac{\gamma M^2 Gr}{Re^2} \theta^{(1)} \frac{\underline{\underline{g}}}{g} . \end{aligned} \tag{62}$$

The condition

$$\frac{\gamma M^2}{Re} \ll 1 \tag{63}$$

is always verified because $M/Re = (\nu_0/c_0)/L$ is the reference Knudsen number (i.e. the ratio between the mean free path ν_0/c_0 and the characteristic length L) that is always much smaller than one in order to satisfy the continuity medium assumption. The condition

$$\frac{\gamma\, M^2\, Gr}{Re^2} \ll 1 \tag{64}$$

may be written as

$$\frac{\gamma\, g\, L}{c_0^2} \ll \frac{1}{\epsilon} \tag{65}$$

that is valid when Eq. (59) is valid provided that $\epsilon < 1$. For liquids $\epsilon < 1$ if $\Delta T < 10^4\, K$. Then, in the EADF Eqs. (63) and (64) may be always used leading to the following expression of the expanded momentum equation

$$\frac{\partial \rho^{(0)}\, \underline{u}^{(0)}}{\partial t} + \nabla^* \cdot \left(\rho^{(0)}\, \underline{u}^{(0)}\, \underline{u}^{(0)}\right) + \nabla\, P^{(0)} = \frac{1}{Re}\, \nabla^* \cdot \underline{\underline{\tau}}^{(0)} - \frac{Gr}{Re^2}\, \theta^{(0)}\, \frac{\underline{\underline{g}}}{g}\,. \tag{66}$$

By collecting the zero-order terms in Eq. (55), one obtains

$$\rho^{(0)}\, C_p^{(0)}\, \frac{D\theta^{(0)}}{Dt} = \frac{1}{Re\, Pr}\, \nabla^* \cdot (\eta^{(0)}\, \nabla\theta^{(0)}) + \frac{Ec}{Re}\, \Phi^{(0)} + Q^{(0)} \tag{67}$$

where Eq. (60) has been employed. The viscous dissipation may be neglected if

$$\frac{Ec}{Re} \ll 1 \tag{68}$$

that means

$$\Delta T \gg \frac{V\, \nu}{C_{p_0}\, L}\,. \tag{69}$$

For liquid flows where $V = 1\, m\, s^{-1}$ and $L = 10\, m$, the lower limit in Eq. (69) is order of $10^{-10}\, ^oC$.

Finally the expanded equation of state (56) is expressed as

$$\rho^{(0)} = 1 - \epsilon\, \theta^{(0)}\,. \tag{70}$$

In Eqs. (61)-(70) the Mach number, the Eckert number and σ have disappeared. Hence, the right-hand sides of Eqs. (43)-(45) and (47) may be expressed as

$$\pi\ (\underline{x}\,,\ t\,,\ Re\,,\ Gr\,,\ Pr\,,\ \epsilon\,)\,. \tag{71}$$

The uniform pressure $p^{(0)}$ accounts for thermodynamic effects while the pressure $P^{(0)}$ appearing in the moment equation accounts for dynamic effects (in Eq. (70) the density does not depend on the dynamic pressure, i.e. the flow is incompressible). The presence of a free surface over which

the pressure is uniform leads to a thermodynamic pressure constant in time and in space. On the contrary, for a closed cavity the thermodynamic pressure $p^{(0)}$ is found to be only spatially uniform, i.e. $p^{(0)} = p^{(0)}(t)$ [6]. Hence the term $p^{(0)}$ must be retained in the equation of state (70) and $p^{(0)}$ is obtained by imposing the conservation of the total mass (i.e. by integrating the continuity equation on the computational domain).

Coming back to the dimensional form and dropping the (0) superscript, the system of governing equations is written as

$$\frac{\partial \rho}{\partial t} + \nabla \cdot (\rho \, \underline{u}) = 0 \,, \tag{72}$$

$$\frac{\partial \rho \, \underline{u}}{\partial t} + \nabla \cdot (\rho \, \underline{u} \, \underline{u}) + \nabla P = \nabla \cdot \underline{\underline{\tau}} + (\rho - \rho_0) \, \underline{g} \,, \tag{73}$$

$$\rho \, C_p \, \frac{DT}{Dt} = \nabla \cdot \underline{q} + Q \,, \tag{74}$$

$$\rho = \rho_0 - \alpha_T \, (T - T_0) \tag{75}$$

where in Eq. (74) the term Q is present only if Eq. (39) is verified.

By defining the variable $\tilde{h}$ as

$$\tilde{h} = \int_{T_0}^{T} C_p \, d\tau + \tilde{h}_0 \tag{76}$$

Eq. (74) may be written as

$$\frac{\partial \rho \, \tilde{h}}{\partial t} + \nabla \cdot (\rho \, \tilde{h} \, \underline{u}) = \nabla \cdot \left(\frac{\eta}{C_p} \nabla \, \tilde{h} \right) + Q \,. \tag{77}$$

For a thermally perfect fluid (like an ideal gas), $\tilde{h}$ coincides with the enthalpy. The enthalpy can be expressed by Eq. (76) also for the EADF case [4]. The system formed by Eqs. (72), (73) and (75) is the one generally employed for liquid flows in commercial CFD codes (e.g. STAR-CD [7] and CFX-4 [8]). Different options are usually available for the type of energy equation to be integrated, being the choice based on the relative importance of the energy contributions[2]. The above analysis has shown that for low Mach numbers both the pressure term and the viscous dissipation term are negligible with respect to the other terms and Eq. (77) could be used.

[2]For example, the total enthalpy equation (Eq. 3) should be integrated when the kinetic energy term is important (high Eckert number), while the static enthalpy equation (Eq. 12) can be used otherwise.

Although the system of governing equations (72)-(75) is closed, Eq. (72) is replaced by an equation for the pressure obtained by making the divergence of the momentum equation and imposing the continuity constrain. It yields (see also Eq. (36))

$$\begin{aligned}\nabla^2 P &= \nabla \cdot \left[-\nabla \cdot (\rho\, \underline{u}\, \underline{u}) + \nabla \cdot \underline{\underline{\tau}} + (\rho - \rho_0)\, \underline{g} \right] \\ &\quad -\frac{\partial}{\partial t} \left[\frac{\beta}{C_p} \left(-\rho\, C_p\, \underline{u} \cdot \nabla T + \nabla \cdot \underline{q} + Q \right) \right] . \end{aligned} \tag{78}$$

Eq. (78) is elliptic showing that acoustic waves have disappeared according to an infinite speed of propagation. Therefore acoustic problems can not be studied by commercial codes.

2.4.1 Oberbeck-Boussinesq equations

Let us consider in Eqs. (61)-(70) the hypothesis of small thermal change, i.e.

$$\frac{T - T_0}{T_0} \ll 1 \tag{79}$$

or

$$\theta^{(0)} \ll \frac{T_0}{\Delta T} . \tag{80}$$

It follows from Eq. (80) that $\epsilon\, \theta^{(0)} \ll \beta_0 T_0$ where in general $\beta_0 T_0 < 1$. Hence, Eq. (70) may be approximated by

$$\rho^{(0)} = 1 \tag{81}$$

and Eqs. (53)-(67) are written to the leading order as

$$\nabla^* \cdot \underline{u}^{(0)} = 0 , \tag{82}$$

$$\frac{\partial \underline{u}^{(0)}}{\partial t} + \nabla^* \cdot \left(\underline{u}^{(0)}\, \underline{u}^{(0)} \right) + \nabla P^{(0)} = \frac{1}{Re} \nabla^* \cdot \underline{\underline{\tau}}^{(0)} - \frac{Gr}{Re^2}\, \theta^{(0)}\, \frac{\underline{g}}{g} , \tag{83}$$

$$C_p^{(0)}\, \frac{D\theta^{(0)}}{Dt} = \frac{1}{Re\, Pr} \nabla^* \cdot \left(\eta^{(0)}\, \nabla \theta^{(0)} \right) + Q^{(0)} \tag{84}$$

where the transport coefficients $\mu^{(0)}$ and $\eta^{(0)}$ are constant. The density variation is retained in the buoyancy term since it is responsible for driving the motion in natural convection problems. The above equations are the *Oberbeck-Boussinesq approximation* of the Navier-Stokes governing equations [3].

When the dimensional analysis is applied to the present flow model, the reference fluid properties β_0 and g do not enter into consideration separately, but only as their product $\beta_0 g$. Therefore Eq. (71) is replaced by $\pi(\underline{x}, t, Re, Gr, Pr)$.

In dimensional form Eqs. (82)-(84) are expressed as

$$\nabla \cdot \underline{u} = 0\,, \tag{85}$$

$$\rho_0 \left[\frac{\partial \underline{u}}{\partial t} + \nabla \cdot (\underline{u}\,\underline{u}) \right] + \nabla P = \nabla \cdot \underline{\underline{\tau}} - \alpha_T \hat{T}\, \underline{g}\,, \tag{86}$$

$$\rho_0 C_p \frac{D\hat{T}}{Dt} = \nabla \cdot \underline{q} + Q \tag{87}$$

where $\hat{T} = T - T_0$. For liquids, the limitations for applying the Oberbeck-Boussinesq approximation is L smaller than few meters (this condition is much more severe than Eq. (59) due to uniform transport coefficients used in the Oberbeck-Boussinesq) and $|\hat{T}|$ of order few degrees only. Therefore it cannot be applied to the modelling of the EADF flows. Anyway, commercial codes do not use this approximation, being their generally formulated with variable density. The Oberbeck-Boussinesq approach is sometimes employed in in-house codes and can be found as an option in CFX-4 [8]).

2.5 EADF Flow Regimes

The system of governing equations (72)-(75) is valid for the mixed convection general case, i.e. when both buoyancy effects and the externally imposed convective field are important.

For the EADF flows, the order of magnitude of the dimensionless numbers may be estimated using the reference values illustrated in Tab. 3. The reference speed V is in general the external

ρ_0	μ_0	η_0	C_{p_0}	c_0	β_0
$kg\,m^{-3}$	$kg\,m^{-1}\,s^{-1}$	$W\,m^{-1}\,K^{-1}$	$J\,kg^{-1}\,K^{-1}$	$m\,s^{-1}$	K^{-1}
10^4	10^{-3}	10	100	10^3	10^{-4}

Table 3: : EADF reference values.

velocity (imposed for instance by a pumping mechanism). When one is interested in the flow around the window, V is the inflow velocity of the part of the circuit that is isolated and simulated. The characteristic fluid velocity inside the EADF is $V = 1\,m\,s^{-1}$. Furthermore, $L = 10\,m$ and

$\Delta T = 100\,K$ if all the circuit is simulated; $L = 10^{-1}\,m$ and $\Delta T = 10\,K$ is for the flow around the window is analysed. Tab. 4 reports the dimensionless numbers for the target and primary circuits and for the flow around the window cases. The Reynolds number is not defined for the target and primary circuits because the flow is uniquely defined by the Grashof number, in the case of pure natural circulation (see next sections). Additional numbers should be considered in the case of gas injection for taking into account the lift force of the bubbles. These numbers would arise from the equation written for a gas-liquid two-phase flow[3].

	Re	Gr	Pr	M	σ	ϵ
target and primary circuits	-	10^{16}	10^{-2}	10^{-3}	10^{-2}	10^{-2}
flow around the window	10^{6}	10^{9}	10^{-2}	10^{-3}	10^{-2}	10^{-3}

Table 4: : Dimensionless numbers for the EADF circuits and for the flow around the window.

2.5.1 Forced convection

Forced convection occurs when the buoyancy term in Eq. (73) is negligible with respect to the inertial term, i.e when $Gr/Re^2 \ll 1$ that may be written as

$$\frac{g\,L\,\beta_0\,\Delta T}{V^2} \ll 1\,. \tag{88}$$

From Tab. 4 it follows that only for the flow around the window Eq. (88) holds and buoyancy effects may be neglected. If we also neglect the influence of the temperature on transport properties (e.g. temperature differences are small), the only relevant flow parameter in Eq. (71) is Re.

2.5.2 Natural convection

A natural convection flow is a flow produced exclusively by buoyancy forces. In this case the reference velocity is not defined as a data of the problem and the value of V to be used in the dimensionless numbers must be obtained as a function of the other flow parameters. This correspond to the EADF circuit where the flow circulation is realised only by means of the heat source term. In this case inertial forces are generated by buoyancy forces only, so they are of the

[3] In the one dimensional case, with the hypothesis of homogeneous bubbles distribution, a number of the type $\rho\,g\,\Delta\rho\,L^3/\mu^2$ would arise from a dimensional analysis, being $\Delta\rho$ the density variation of the lead-bismuth due to the bubbles injected in the rising duct of length L. The relative importance of bubbles pumping and natural convection could be evaluated by comparing this number with the Grashof number.

same order of magnitude, i.e. $Gr/Re^2 = 1$. This implies that the characteristic velocity is given by

$$V^2 = g\, L\, \beta_0\, \Delta T\,. \tag{89}$$

Hence Eq. (66) is written as

$$\frac{\partial \rho^{(0)}\, \underline{u}^{(0)}}{\partial t} + \nabla^* \cdot \left(\rho^{(0)}\, \underline{u}^{(0)}\, \underline{u}^{(0)}\right) + \nabla\, P^{(0)} = \frac{1}{Gr^{1/2}}\, \nabla^* \cdot \underline{\underline{\tau}}^{(0)} - \theta^{(0)}\, \frac{\underline{\underline{g}}}{g}\,. \tag{90}$$

Here the square root of the Grashof number represents the ratio between inertial and viscous forces. Therefore, when the Grashof number is large viscous forces are negligible with respect to inertial forces (however they can not be neglected in the near wall region). On the other hand, when Gr is small viscous forces are important in all the domain.

The energy equation (67) is written as

$$\rho^{(0)}\, C_p^{(0)}\, \frac{D\theta^{(0)}}{Dt} = \frac{1}{Gr^{1/2}\, Pr}\, \nabla^* \cdot (\eta^{(0)}\, \nabla\theta^{(0)}) + Q^{(0)}\,. \tag{91}$$

For natural convection Re disappears from Eq. (71) and Gr may be replaced by the Rayleigh number $Ra = Gr\, Pr$.

This is the case for the global analysis of the target and primary circuits (when gas injection is not considered). Fixed all the other circuit's characteristics, the flow regime is uniquely defined by the Grashof number based on the height of the circuit and on the mean temperature difference between the rising and the downcoming ducts.

2.5.3 Mixed convection

When a piece of the EADF circuit is isolated and analysed, we have a situation where an external velocity is imposed (as a consequence of the global circulation). If local buoyancy effects are negligible in the considered piece of circuit, we are in the case of forced convection. However, in the spallation region of the target (flow around window), strong local temperature gradients occur, driving a local natural convection which could compete with the local forced convection. This flow regime is called mixed convection.

In this case the Reynolds number is based on the externally imposed velocity V, while Gr is based on the local temperature differences. The ratio Gr/Re^2 gives the order of magnitude of the buoyancy forces with respect to the inertial forces generated by forced convection. When $Gr/Re^2 = 1$, the two effects are comparable.

From Tab. (4), this ratio in the spallation region is equal to 10^{-3} and local natural convection could be neglected. However, this is the situation at the highest flow rate. At lower flow rates or in transient conditions, the effect of local buoyancy could become very important.

3 Numerical Solution Techniques

In the following, a brief review of the solution techniques commonly used in CFD codes is presented. The pressure-based formulation is generally used in commercial codes. This formulation is especially suitable for low Mach number (incompressible) flows and can be adapted to the case of compressible flows. Another method is based on the extension of the density based approach, suitable for compressible flows, to the low Mach number case through preconditioning techniques.

Both these formulations and all the models presented in the following can be applied to liquid metal flows of interest for the EADF activity.

3.1 General Form of Governing Equations

The system of governing equations (72), (73) and (77) may be expressed in conservative form as

$$\frac{\partial \mathcal{W}}{\partial t} + \nabla \cdot (\mathcal{F}_E - \mathcal{F}_V) = \mathcal{S} \tag{92}$$

where

$$\mathcal{W} = \begin{bmatrix} \rho \\ \rho\,\underline{u} \\ \rho\,\tilde{h} \end{bmatrix}, \qquad \mathcal{F}_E = \begin{bmatrix} \rho\,\underline{u} \\ \rho\,\underline{u}\,\underline{u} + P\,\underline{\underline{I}} \\ \rho\,\tilde{h}\,\underline{u} \end{bmatrix}, \qquad \mathcal{F}_V = \begin{bmatrix} 0 \\ \underline{\underline{\tau}} \\ \underline{q} \end{bmatrix}, \qquad \mathcal{S} = \begin{bmatrix} 0 \\ 0 \\ Q \end{bmatrix}.$$

The density is related to the temperature by means of Eq. (75). Furthermore, initial and boundary conditions are given by Eq. (28) and Eqs. (31)-(33) respectively.

Eqs. (92) have the form of the convection-diffusion equation

$$\frac{\partial \rho\,\phi}{\partial t} + \nabla \cdot (\,\rho\,\phi\,\underline{u} - \Gamma\,\nabla\phi\,) = S\,. \tag{93}$$

In particular, the continuity equation is obtained by assigning $\phi = 1$ and $S = 0$, while for the momentum equation ($\phi = \underline{u}$) and the energy equation ($\phi = \tilde{h}$) one has respectively

$$\Gamma = \mu\,, \quad S = \nabla \cdot \left[\,\mu\,\nabla\underline{u}^T - P\,\underline{\underline{I}}\,\right] \tag{94}$$

and

$$\Gamma = \frac{\eta}{C_p}\,, \quad S = Q \tag{95}$$

(if Eq. (16) is used, then $S = -\beta T Dp/Dt + \Phi + Q$). In the present work laminar equations are considered. When turbulence is accounted for by applying the Reynolds averaging and using Boussinesq closures [7], in Eqs. (92) the following modifications must be introduced: (i) all the

quantities are replaced by their mean values; (ii) the transport coefficients Γ include the eddy-viscosity contributes; (iii) the pressure P and $\tilde{h}$ include additional terms related to the turbulent kinetic energy of the flow. Furthermore, when a $k-\varepsilon$ model is employed one has to integrate two additional transport equations whose form is still represented by Eq. (93). Therefore, by taking into account such modifications the extension to turbulent flows of the numerical models illustrated in the following is straightforward.

3.2 Pressure Based Numerical Methods

The Finite Volume method is the approach commonly used in CFD commercial codes. The cells of the computational mesh are considered as control volumes where the conservation equations are integrated. By applying the Gauss theorem to the divergence-form terms, the integration of the generic Eq. (93) over the computational cell leads to the discretised equation

$$\Delta V_P \frac{d(\rho\phi)_P}{dt} = -\sum_m \left(\rho\,\phi\,\underline{u} - \Gamma\,\nabla\phi\right)_m \cdot \underline{A}_m + S_P\,\Delta V_P \tag{96}$$

where ΔV_P is the volume of the computational cell and the m-subscript runs on cell-faces. For the m-cell-face, $|\underline{A}_m|$ is the area and $\underline{n} = \underline{A}_m/|\underline{A}_m|$ the outgoing normal. The value of the variables is assigned to the cell centre and is denoted as $(\cdot)_P$.

The terms

$$\begin{aligned} F_c &= -\sum_m \left(\rho\,\phi\,\underline{u}\right)_m \cdot \underline{A}_m \\ F_v &= \sum_m \left(\Gamma\,\nabla\phi\right)_m \cdot \underline{A}_m \end{aligned}$$

are the convective and diffusive fluxes respectively. They must be calculated on the cell faces by using the value of the variable in the cell centre ϕ_P and the values in the centre of the neighboring cells ϕ_{nb}, the way this is done depending on the discretisation scheme used (see Sec. 3.2.1). The result of this discretisation practice can be always written in the form

$$Fc + Fv = -\hat{a}_P\,\phi_P + \sum_{nb} \hat{a}_{nb}\,\phi_{nb} \tag{97}$$

where the the coefficients $\hat{a}_P$ and $\hat{a}_{nb}$ are functions of the density, velocity and diffusion coefficients in the considered cell and in its neighboring cells.

The form of the source term $S_P\,\Delta V_P$ depends on the considered variable and circumstances. However, it can be always expressed as a quasi-linear function of ϕ_P as

$$S_P\,\Delta V_P = S_u + S_p\,\phi_P \tag{98}$$

where S_u and S_p are analogous to the $\hat{a}$ coefficients for the flux terms.

In the stationary case, we have

$$\Delta V_P \, \frac{d(\rho\phi)_P}{dt} = 0$$

and the discretised Eq. (96) becomes

$$\hat{a}_P \, \phi_P = \sum_{nb} \hat{a}_{nb} \, \phi_{nb} + S_u \tag{99}$$

having included the S_p term in the $\hat{a}_P$ matrix. Eq. (99) is a quasi-linear system which can be solved with the methods described in Sec. 3.2.2, yielding the ϕ field relative to the considered values of the $\hat{a}$ coefficients, which depend on the value of the other flow variables. For the solution of the stationary flow field, a system of equations of the type (99) (one for every flow variable) has to be solved, using the iterative procedures described in Sec. 3.2.3. In the following, the iterations relative to the solution of the field equations are indicated with the ν subscript.

In the non-stationary case, assuming constant density, the inertial term can be written as

$$\Delta V_P \, \frac{d(\rho\phi)_P}{dt} = \rho \, \Delta V_P \, \frac{\phi_P^\nu - \phi_P^0}{\Delta t}$$

and Eq. 99 becomes

$$\rho \, \Delta V_P \, \frac{\phi_P^\nu - \phi_P^0}{\Delta t} + \hat{a}_P \, \phi_P^\nu = \sum_{nb} \hat{a}_{nb} \, \tilde{\phi}_{nb} + S_u \tag{100}$$

where

$$\tilde{\phi} = \theta \, \phi^\nu + (1 - \theta) \, \phi^0 \qquad (0 \leq \theta \leq 1) \tag{101}$$

and the superscripts ν and 0 refer to the time $t_n + \Delta t$ and t_n respectively. In this case, the ν-iterative process leads the solution from the time t_n to the time $t_n + \Delta t$. The iterative process is necessary because Eq. (96) is linearised by calculating the matrix coefficients as functions of given density, velocity and diffusion coefficients (the fields at the $(\nu - 1)$-iteration). The solution may be obtained avoiding the ν-iterative process if a sufficiently small Δt is used (in this case the linearisation error may be neglected).

In Eq. (101) the values $\theta = 0$, $\theta = 1/2$ and $\theta = 1$ correspond to the explicit, Crank-Nicholson and implicit scheme respectively. It can be shown that the implicit scheme is the only one that does not require a stability condition on the time-step [8]. Nevertheless, the unconditionally stable implicit scheme is only first-order accurate in time with respect to the second-order Crank-Nicholson scheme. Second-order in time may be obtained with the implicit scheme by using the discretization of the inertial term given by [9]

$$\frac{d\phi_P}{dt} = \frac{3/2 \, \phi_P^\nu - 2 \, \phi_P^0 + 1/2 \, \phi_P^{n-1}}{\Delta t} \tag{102}$$

where ϕ^{n-1} refers to the time $t_n - \Delta t$. We will concentrate on the first-order implicit scheme ($\theta = 1$) that is robust and unconditionally stable even if small time-steps are necessary in time-dependent computations to ensure the accuracy of results.

For non-constant density flows, Eq. (96) may be approximated using the zero-order linearisation in terms of density given by

$$\frac{d(\rho\phi)_P}{dt} = \rho_P^{\nu-1}\,\frac{\phi_P^{\nu} - \phi_P^0}{\Delta t}\,. \tag{103}$$

Hence in general Eq. (100) may be written as

$$a_P\,\phi_P = \sum_{nb} a_{nb}\,\phi_{nb} + b \tag{104}$$

where the superscript ν has been dropped and

$$a_P = \hat{a}_P + a_P^0 \tag{105}$$

$$a_{nb} = \hat{a}_{nb} \tag{106}$$

$$b = S_u + a_P^0\,\phi_P^0 \tag{107}$$

being

$$a_P^0 = \begin{cases} \rho_P^{\nu-1}\,\dfrac{\Delta V_P}{\Delta t} & \text{for unsteady flows} \\ 0 & \text{for steady flows.} \end{cases} \tag{108}$$

Eq. (104) has the same form of Eq. (99), the only difference being in the expressions of the coefficients. Therefore, the same solution algorithms can be used for both the steady and the transient forms of the equations.

3.2.1 Spatial Discretization

As explained in Sec. 3.2, an expression for the convective and diffusive fluxes across the cell faces as a function of the values on the cell centers is needed. This operation is called spatial discretisation.

The diffusive term of Eq. (96) is elliptic, which means that it is equally influenced by all the values in the surrounding cells. The discretisation of this term is not a problem, and centered schemes are usually employed. On the contrary, the stability and the accuracy of the numerical solution depends on the discretisation scheme used for the convective terms. In the following, the

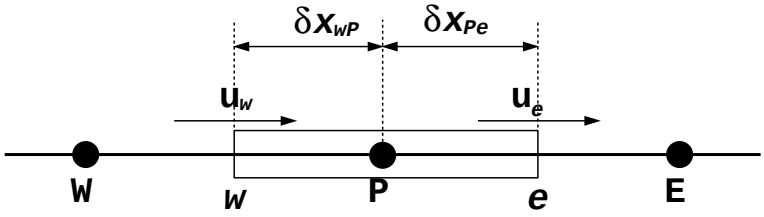

Figure 1: One dimensional computational grid.

most common spatial discretisation techniques are presented in their one dimensional formulation on a uniform grid.

Fig. 1 shows the one dimensional computational cell. The value of the convective flux $\rho\,\phi\,u$ has to be calculated on the two faces w and e of the cell.

Central differencing

In the central differencing scheme the fluxes are calculated as

$$(\rho\,\phi\,u)_w = \frac{1}{2}\left[(\rho\,\phi\,u)_W + (\rho\,\phi\,u)_P\right] \tag{109}$$

$$(\rho\,\phi\,u)_e = \frac{1}{2}\left[(\rho\,\phi\,u)_P + (\rho\,\phi\,u)_E\right] \quad . \tag{110}$$

This scheme is second order accurate. However it can be shown that, due to its inability to identify flow direction, it can be unstable when the convective fluxes are dominant on the diffusive fluxes [10]. A measure of the relative importance of convection with respect to diffusion is given by the Peclet number, defined as

$$Pe = \frac{\rho\,u}{\Gamma/\delta x} \quad , \tag{111}$$

being δx the characteristic cell dimension. The central differencing scheme is stable when the Peclet number calculated on the cell face is greater than 2 [10].

Upwind differencing

The upwind differencing scheme takes into account the flow direction, assigning the value at the upstream node as the convected value of ϕ at a cell face. For the case in Fig. 1, where the velocity has the w-e direction, we have

$$(\rho\,\phi\,u)_w = (\rho\,\phi\,u)_W \tag{112}$$

$$(\rho\,\phi\,u)_e = (\rho\,\phi\,u)_P \quad . \tag{113}$$

The upwind scheme is first order accurate, but is always stable. It is said to be very diffusive, in the sense that it introduces an error that behaves like a diffusion term (numerical diffusion), resulting in a smearing of the solution.

Hybrid differencing

The hybrid differencing scheme is a combination of the central and upwind differencing schemes. Considering for example the w face, the hybrid scheme switches from the upwind or to the central scheme on the basis of the value of the Peclet number on the cell face:

$$(\rho\,\phi\,u)_w = (\rho\,\phi\,u)_W \qquad \text{when} \qquad Pe > 2 \tag{114}$$

$$(\rho\,\phi\,u)_w = \frac{1}{2}\left[(\rho\,\phi\,u)_W + (\rho\,\phi\,u)_P\right] \qquad \text{when} \qquad Pe < 2. \tag{115}$$

$$\tag{116}$$

Higher order schemes

Among the higher order schemes, the QUICK differencing scheme [10] is more accurate than the central and hybrid schemes also if undershoots and overshoots may be present in the solution. Other schemes as the Total Variation Diminishing (TVD) schemes are specially formulated to achieve oscillation-free solutions at the cost of an increased computational effort.

All the schemes described above can be extended to the three dimensional case in body-fitted grids, still maintaining their general characteristics. The expression of the coefficients of Eq. (104) depends on the chosen discretisation technique.

In general, for an accurate calculation, second or higher order schemes should be used for the discretisation of momentum and energy equations. The upwind scheme can be used for the turbulent equations in order to increase their numerical stability.

3.2.2 Solution of the Linear System

The linear system (104) can be solved using different approaches. Direct inversion of the matrix is in general too expensive. Then, iterative algorithms are usually employed. The *Gauss-Seidel method* consists in solving

$$\phi_P = \frac{\sum_{nb}\, a_{nb}\,\phi_{nb} + b}{a_P} \tag{117}$$

where ϕ_{nb} stands for the neighbor values present in the computer storage. The *line-by-line method* used in Ref. 8 is a combination of the Gauss-Seidel method and of the *Tri-Diagonal Matrix Algorithm (TDMA)* direct method. Other iterative techniques are the line-by-line *Alternating-Direction Implicit (ADI)*, the *Incomplete Lower-Upper Decomposition (ILU)*, the *Strongly Implicit Procedure (SIP)*, the *Conjugate Gradient (CG)* that includes the *Generalised Minimal Residual (GMRES)*, the *Bi-Conjugate Gradient (Bi-CG)*, the *Conjugate Gradient Square (CGS)* and the *Bi-CGSTAB* [8,10].

In general the iterative solution of the algebraic equations need not to be taken to complete convergence in the intermediate state of the ν iterations.

Although commercial codes allow the choice of the solution method for the linear system, the default option is usually suitable for any application.

3.2.3 Solution Algorithms

The Semi-Implicit Method for Pressure-Linked Equations (SIMPLE) is generally employed in commercial codes (e.g. STAR-CD and CFX) to integrate the governing equations. In this method the discretized continuity, momentum and energy equations (104) are solved with a sequential procedure where the momentum equation is used to obtain an approximated velocity field that is then corrected in order to satisfy mass conservation. Eq. (104) written for the momentum equation yields

$$a_P \, \underline{u}_P^* = \sum_{nb} a_{nb} \, \underline{u}_{nb}^* - \Delta V_P \, (\nabla P^*)_P + \underline{b} \tag{118}$$

where the discretized pressure gradient has not been included in the source term $\underline{b}$ and P^* is a guessed pressure field, e.g the pressure at the the previous iteration so that $P^* = P^{\nu-1}$. In the Finite Volume approach cell-centre gradients are calculated, using the Gauss theorem, as

$$\Delta V_P \, (\nabla P^*)_P = \sum_{m} P_m^* \, \underline{A}_m \, . \tag{119}$$

The velocity field $\underline{u}^*$ calculated by Eq. (118) does not satisfy the continuity equation and must be corrected by a pressure field calculated using the continuity equation that acts as a constraint for momentum [8]. The velocity field $\underline{u}$ that satisfies the continuity equation at the iteration ν and the corresponding pressure fields P are solutions of the equation

$$a_P \, \underline{u}_P = \sum_{nb} a_{nb} \, \underline{u}_{nb} - \Delta V_P \, (\nabla P)_P + \underline{b} \, . \tag{120}$$

By subtracting Eq. (118) from Eq. (120), the equation for the velocity correction

$$\underline{u}'_P = \underline{u}_P - \underline{u}_P^* \tag{121}$$

is obtained in terms of the pressure correction

$$P'_P = P_P - P_P^* \, . \tag{122}$$

It yields

$$\underline{u}_P = \underline{u}_P^* - \frac{\Delta V_P}{a_P} \, (\nabla P')_P \tag{123}$$

where the term $\sum_{nb} a_{nb}\underline{u}'_{nb}$ has been neglected. A formula similar to Eq. (123) can be derived for the velocity on cell faces. This formula, substituted into the discretised continuity equation, given by

$$\sum_{m}(\rho\,\underline{u}\,A) = 0 \tag{124}$$

gives an equation for the pressure correction P' of the form

$$a'_P\,P'_p = \sum_{nb} a'_{nb}\,P'_{nb} + b'_P \quad . \tag{125}$$

The source term b'_P is the mass imbalance arising from the incorrect velocity field u^*.

The procedure of the SIMPLE method is the following [8].

1 Starting from a guess pressure field P^* solve Eq. (118) to obtain $\underline{u}^*$.

2 Solve the pressure-correction equation (125) for P'.

3 Calculate P from Eq. (122).

4 Calculate the velocity field $\underline{u}$ from Eq. (123).

5 If it is necessary solve Eq. (104) for other scalars.

6 Treat P as the new P^* and return to step 1.

It is important to note that the approximations made in deriving Eqs. (123) do not alter the converged solution. In fact at convergence the relations $\underline{u}' = 0$ and $P' = 0$ give values of P and $\underline{u}$ that always satisfy the discretized momentum and continuity equations. Furthermore, the convergence is achieved via a series of continuity-satisfying velocity fields that help the convergence of other transported scalars (e.g. the turbulence kinetic energy and dissipation when the $k-\varepsilon$ model is used).

In the derivation of the pressure-correction equation no dependence of pressure on density has been considered (the equation is linearized in terms of velocity and density fields). This approximation is justified by the iterative essence of the method at least when solving for incompressible flows, when the effect of pressure on velocity is of primary importance. Vice versa, in highly compressible flows (e.g. supersonic) the effect of pressure on density is of primary importance and there is possibility of divergence due to the strong non-linearity. For compressible flows a "compressible" form of Eq. (125) should be derived (e.g. by linearizing the density as function of pressure in the expressions of the matrix coefficients).

In order to improve the SIMPLE method, some revised version have been proposed. Among them there are SIMPLER, SIMPLEC and PISO (see Ref. 8 and 10).

Convergence Criteria

In the uncoupled approach, a residual $\mathcal{R}$ may be computed for each equation (momentum, pressure, energy and scalars) in each cell. It reads

$$\mathcal{R} = \sum_{nb} a_{nb}\,\phi_{nb} + b - a_P\,\phi_P\,. \tag{126}$$

Convergence criteria are usually formulated by imposing that for each equation the largest value or the norm of $|\mathcal{R}|/\mathcal{R}_{ref}$ in the computational domain be less than a certain small number. For flows with inlets the reference value $\mathcal{R}_{ref}$ is assumed equal to the inlet flux; for enclosed domains, $\mathcal{R}_{ref}$ is taken as the residual after a fixed number of iterations. Also the mass source represents a valid indicator of the convergence of the solution.

3.2.4 Relaxation techniques

Several relaxation techniques may be used in order to accelerate or stabilise the convergence process.

Relaxation on variable

In this relaxation strategy, once the linear system has been solved, the variable ϕ is corrected by using

$$\phi_P^{new} = \alpha\,\phi_P + (1-\alpha)\,\phi_P^{\nu-1} \tag{127}$$

where α is a constant less than one (under-relaxation). Often, density, diffusion coefficients and source terms are also under-relaxed by using Eq. (127).

Pseudo-transient relaxation

Eq. (104) is replaced by

$$\phi_P = \alpha\,\frac{\sum_{nb}\ a_{nb}\,\phi_{nb} + b}{a_P} + (1-\alpha)\,\phi_P^{\nu-1} \tag{128}$$

or

$$\frac{a_P}{\alpha}\,\phi_P = \sum_{nb} a_{nb}\,\phi_{nb} + b + \frac{1-\alpha}{\alpha}\,a_P\,\phi_P^{\nu-1}\,. \tag{129}$$

The diagonal predominance of the system formed by Eqs. (129) is greater with respect to Eq. (104) if α is a constant less than one (under-relaxation).

Solving the unsteady form of Eq. (104) with no inner iterative process is equivalent to solve the steady form of Eq. (129) with a cell-varying under-relaxation parameter given by

$$\alpha = \frac{\hat{a}_P}{\hat{a}_P - a_P^0} \,. \tag{130}$$

Eq. (129) may be used for unsteady computations: in this case the inner ν-iterations are under-relaxed.

Relaxation of the linear system

When solving iteratively the linear system, the change from iteration to iteration in the values of dependent variables may be accelerated or slowed down by using over-relaxation or under-relaxation respectively. Over-relaxation or under-relaxation are achieved by using $\alpha > 0$ and $\alpha < 0$ respectively in

$$\phi_P^r = \alpha\, \phi_P^r + (1-\alpha)\, \phi_P^{r-1} \tag{131}$$

where ϕ_P^r comes from the solution of Eq. (104) and r is the index of the iterative algorithm solving the linear system.

Usually, in the SIMPLE method, the under-relaxation (129) on Eq. (118) and the under-relaxation

$$P = P^* + \alpha_p\, P' \tag{132}$$

on Eq. (122) is applied. Therefore, the parameters α in Eqs. (129) and (132) are the "relaxation coefficients" to be given as input in commercial codes.

3.3 Density-Based Numerical Methods

Time-marching density-based codes have been successfully used for solving hyperbolic systems obtained when discretising compressible flow governing equations. These codes have become highly sophisticated in terms of geometry complexity, accurate spatial discretization and convergence acceleration techniques[12,13]. Such methods perform the time-integration of the conserved variables by Runge-Kutta explicit algorithms or by implicit algorithms (e.g. Approximate Factorization and LU decomposition). For the spatial discretization of the convective fluxes high order schemes have been developed (e.g. Artificial Dissipation, TVD symmetric or upwind, MUSCL, ENO). Local time-stepping, implicit residual smoothing and multigrid are often used to accelerate the convergence. However, numerical algorithms developed for compressible flows are often ineffective when the Mach number is reduced because of the stiffness of the system's eigenvalues. In

fact, the time-step is limited for stability reasons by the largest eigenvalue which, for low speeds, is approximately the speed of sound. When the Mach number approaches zero the convergence slows dramatically due to the disparity of the wave speeds. In recent years, preconditioning methods have been used to eliminate the eigenvalues stiffness at low speed. The major advantage of the preconditioning methods is that they may be easily implemented into existing time-marching compressible codes whose peculiarities are retained.

Furthermore, preconditioning methods allow to solve a further difficulty that arises when trying to simulate incompressible flows using density-based algorithms. Following the cell-centred Finite Volume approach the system of governing equations (92) is written in compact form as

$$\Delta V_P \frac{d\mathcal{W}_P}{dt} = -\sum_m \left(\mathcal{F}_E - \mathcal{F}_V\right)_m \cdot \underline{A}_m + \mathcal{S}_P \Delta V_P \,. \tag{133}$$

Time-marching schemes update the conserved variable term $\mathcal{W}$ making impossible to evaluate the pressure P (P does not compare both in $\mathcal{W}$ and in the equation of state). Then, by introducing the matrix

$$\mathcal{K} = \begin{bmatrix} 1 & 0 & 0 \\ -\underline{u} & \underline{\underline{I}} & 0 \\ -\tilde{h} & 0 & 1 \end{bmatrix}$$

the system (133) is transformed in the non-conservative form

$$\Delta V_P \left(\mathcal{K}\frac{\partial \mathcal{W}}{\partial \mathcal{Q}}\right)_P \frac{d\mathcal{Q}_P}{dt} = -\mathcal{K}_P \left[\sum_m \left(\mathcal{F}_E - \mathcal{F}_V\right)_m \cdot \underline{A}_m + \mathcal{S}_P \Delta V_P\right] . \tag{134}$$

where $\mathcal{Q} = \left[P, \underline{u}, \tilde{h}\right]^T$ is the vector of the primitive variables. In the matrix

$$\mathcal{K}\frac{\partial \mathcal{W}}{\partial \mathcal{Q}} = \begin{bmatrix} 0 & 0 & \partial\rho/\partial\tilde{h} \\ 0 & \rho\,\underline{\underline{I}} & 0 \\ 0 & 0 & \rho \end{bmatrix}$$

the term $(1,1)$ that multiplies the time-derivative of pressure controls the pressure wave speeds and is responsible of the eigenvalues' stiffness. Preconditioning methods are based on the technique developed by Chorin [14]: an artificial compressibility term under the form of a time-derivative of pressure replaces the time-derivative of density in the continuity equation. Therefore, the continuity equation (1) is replaced by

$$\frac{1}{v^2}\frac{\partial P}{\partial t} + \nabla \cdot (\rho\,\underline{u}) = 0 \tag{135}$$

and consequently $\mathcal{K}\partial\mathcal{W}/\partial\mathcal{Q}$ is replaced by the matrix [15]

$$\mathcal{P}^{-1} = \begin{bmatrix} \frac{1}{\upsilon^2} & 0 & 0 \\ 0 & \rho\,\underline{\underline{I}} & 0 \\ 0 & 0 & \rho \end{bmatrix}$$

where υ is the artificial-compressibility parameter that represents the pressure wave speed of the preconditioned system. Hence, Eqs. (134) are replaced by

$$\Delta V_P \frac{d\mathcal{Q}_P}{dt} = -(\mathcal{P}\,\mathcal{K})_P \left[\sum_m (\mathcal{F}_E - \mathcal{F}_V)_m \cdot \underline{A}_m + \mathcal{S}_P\,\Delta V_P \right] \tag{136}$$

where

$$\mathcal{P}\,\mathcal{K} = \begin{bmatrix} \upsilon^2 & 0 & 0 \\ -\underline{u}/\rho & \underline{\underline{I}}/\rho & 0 \\ -\tilde{h}/\rho & 0 & 1/\rho \end{bmatrix} . \tag{137}$$

In Eqs. (136) the pressure P is updated by its time-derivative and the equation of state (75) is employed to obtain the density.

By defining $f = \mathcal{F}_E \cdot \underline{n}$, the eigenvalue of $\mathcal{A} = \mathcal{P}\,\mathcal{K}\partial f/\partial\mathcal{Q}$ are

$$\lambda_r(\mathcal{A}) = U\,,\ U\,,\ U\,,\ U/2 + c\,,\ U/2 - c \tag{138}$$

where $U = \underline{u} \cdot \underline{n}$ and $c = \sqrt{(U/2)^2 + \upsilon^2}$. Usually υ may be given by an expression as

$$\upsilon^2 = max(\upsilon_0^2\,,\ \underline{u} \cdot \underline{u}) \tag{139}$$

where υ_0 is a constant greater than zero in order to ensure that one eigenvalue is negative for subsonic flows. The value of υ is critical for the convergence properties of the method. Actually, well-conditioned λ_r are obtained when υ makes the pseudo acoustic wave speed of the same order of the particle velocity. By increasing υ, pressure-waves field adjusts faster but the bad-conditioning of the inviscid eigenvalues grows up, especially in presence of large recirculation zone where the velocity of fluid is small. Nevertheless, when the Reynolds number decreases the characteristic time of viscosity spreading also decreases and if υ is too small the boundary layer can not adapt to the too slowly developing pressure field and fluctuations of separation regions may destroy the convergence. [8]

Different methods based on the artificial compressibility technique have been suggested. A perturbed form of the governing equations may be obtained by expanding the flow variables in

terms of the Mach number [16]. Alternatively, preconditioning matrixes as (137) are developed in order to re-scale the eigenvalues to the same order of magnitude [8,16-17]. Recently, the preconditioning approach has been proposed to solve reacting and non reacting flows within a wide Mach number range. [18-20]

The density based preconditioned approach is less expensive from the computational point of view. However, it could be less robust than the pressure based approach, and requires skill users for an efficient performance. This is the main reason why it is not adopted in commercial CFD codes.

The CRS4 in-house code KARALIS is based on the above procedure. It will be used in the EADF computation activity and its performance will be compared with that of commercial codes in the near future.

4 Conclusions

The fluid-dynamic modelling for the simulation of the Lead-Bismuth flow in the EADF was reviewed. The general form of the non-dimensional governing equation was derived, and the analysis of the orders of magnitude of the different terms in the case of a the liquid metal flows in the EADF was performed, through a low-Mach number asymptotic analysis. It was found that the resulting form of the equations is the one commonly used in commercial CFD codes for the simulation of liquid flows, which can then be used for our applications.

The most common numerical methods for low-Mach number applications were also presented. These methods are general and can be applied to liquid metal flows without any modification.

The peculiarity of the numerical simulation of liquid metal flows lies in the modelling of the turbulent heat transfer, due to the low Prandtl number of this type of fluids. This subject is discussed in [21].

References

[1] Ansaldo, CRS4, ENEA, INFN, "Energy Amplifier Demonstration Facility: Reference Configuration", EA B0.00 1 199 - Rev. 0, December 1998.

[2] Batchelor, G.K., *An Introduction to Fluid Dynamics*, Cambridge University Press, Cambridge, 1967.

[3] Landau, L.D., and Lifshitz, E.M., *Fluid Mechanics*, Pergamon Press, Oxford, 1989.

[4] V. Bellucci, S. Buono, G. Fotia, L. Maciocco, V. Moreau, M. Mulas, G. Siddi, L. Sorrentino, *Phenomenology of Liquid Metal Thermal-Hydraulics*, CRS4 Technical Report 99/12, Cagliari, 1999.

[5] Barenblatt, G.I., *Scaling, Self-Similarity, and Intermediate Asymptotics*, Cambridge University Press, Cambridge, UK, 1996.

[6] Paolucci, S., "On the Filtering of Sound from the Navier-Stokes Equations", Report No. SAND82-8257, Sandia National Laboratories, Livermore, CA, 1987.

[7] Tennekes, H., and Lumley, J.L., *A First Course in Turbulence*, The MIT Press, Cambridge, 1872.

[8] Patankar, S.V., *Numerical Heat Transfer and Fluid Flow*, Hemisphere Publishing Co., New York, 1980.

[9] Rogers, S.E., and Kwack, D., "Steady and Unsteady Solutions of the Incompressible Navier-Stokes Equations", *AIAA Journal*, Vol. 29, 1991, pp. 603-610.

[10] Versteeg, H.K., and Malalasekera, W., *An Introduction to Computational Fluid Dynamics*, Longman, Edinburgh, 1995.

[11] Rhie, C.M., and Chow, W.L., "Numerical Study of the Turbulent Flow Past an Airfoil with Trailing Edge Separation", *AIAA Journal*, Vol. 21, 1983, pp. 1525-1532.

[12] Martinelli, L., "Calculations of Viscous Flows with a Multigrid Method", Ph.D. Thesis, MAE Department, Princeton Univ., Princeton, NJ, Oct. 1987.

[13] Yee, H.C., "A Class of High-Resolution Explicit and Implicit Shock-Capturing Methods", NASA TM-101088, 1989.

[14] Chorin, A.J., "A Numerical Method for Solving Incompressible Viscous Flow Problems", *Journal of Computational Physics*, Vol. 2, 1967, pp. 12-26.

[15] Turkel, E., "Preconditioning Methods for Solving the Incompressible and Low Speed Compressible Equations", *Journal of Computational Physics*, Vol. 72, 1987, pp. 277-298.

[16] Merkle, C.L., and Choi, Y.-H., "Computation of Low-Speed Compressible Flows with Time-Marching Procedures", *International Journal for Numerical Methods in Engineering*, Vol. 25, 1988, pp. 293-311.

[17] van Leer, B., Lee, W.T., and Roe, P.L., "Characteristic Time Stepping or Local Preconditioning of the Euler Equations", AIAA Paper 91-1552, 1991.

[18] Choi, Y.-H., and Merkle, C.L., "The Application of Preconditioning in Viscous Flows", *Journal of Computational Physics*, Vol. 105, 1993, pp. 207-223.

[19] Shuen, J.-S., Chen, K.-H., and Choi, Y., "A Coupled Implicit Method for Chemical Non-equilibrium Flows at All Speeds", *Journal of Computational Physics*, Vol. 106, 1993, pp. 306-318.

[20] Dailey, L., and Pletcher, R., "Evaluation of Multigrid Acceleration for Precondiotioned Time-Accurate Navier-Stokes Algorithms", AIAA Paper 95-1668, 1995.

[21] V. Bellucci, S. Buono, G. Fotia, L. Maciocco, V. Moreau, M. Mulas, G. Siddi, L. Sorrentino, *Turbulence Models in the Numerical Analysis of Liquid Metal Systems*, paper in preparation.